

1 **Evidence of a prolonged drought ca. 4200 yr BP**
2 **correlated with prehistoric settlement abandonment**
3 **from the Gueldaman GLD1 Cave, N-Algeria**

4

5 **J. Ruan^{1,5}, F. Kherbouche², D. Genty¹, D. Blamart¹, H. Cheng^{3,4}, F.**
6 **Dewilde¹, S. Hachi², R. L. Edwards⁴, E. Régnier¹ and J.-L. Michelot⁵**

7 ¹Laboratoire des Sciences du Climat et de l'Environnement, Gif-sur-Yvette, France

8 ²Centre National de Recherches Préhistoriques, Anthropologiques et Historiques,
9 Algiers, Algeria

10 ³Institute of Global Environmental Change, Xi'an Jiaotong University, Xi'an, China

11 ⁴Department of Geological Sciences, University of Minnesota, Minnesota, USA

12 ⁵Laboratoire Géosciences Paris Sud, UMR 8148, Université Paris-Sud, Orsay, France

13 Correspondence to: J. Ruan (jiaoyangruan@gmail.com)

14

15 **Abstract**

16 Middle Holocene cultures have been widely studied around the E-Mediterranean
17 basin in the last 30 years and past cultural activities have been commonly linked with
18 regional climate changes. However, in many cases such linkage is equivocal, in part
19 due to existing climatic evidence that has been derived from areas outside the
20 distribution of ancient settlements, leading to uncertainty from complex spatial
21 heterogeneity in both climate and demography. A few high-resolution well-dated
22 paleoclimate records were recently established using speleothems in the Central and
23 E-Mediterranean basin, however, the scarcity of such records in the western part of
24 the Mediterranean prevents us from correlating past climate evolutions across the
25 basin and deciphering climate-culture relation at fine time scales.

1 Here we report the first decadal-resolved Mid-Holocene climate proxy records from
2 the W-Mediterranean basin based on the stable carbon and oxygen isotopes analyses
3 of two U/Th dated stalagmites from the Gueldaman GLD1 Cave in N-Algeria.
4 Comparison of our records with those from Italy and Israel reveals synchronous
5 (multi) centennial dry phases centered at ca. 5600 yr BP, ca. 5200 yr BP and ca. 4200
6 yr BP across the Mediterranean basin. New calibrated radiocarbon dating constrains
7 reasonably well the age of rich anthropogenic deposits (e.g., faunal remains, pottery,
8 charcoal) excavated inside the cave, which allows the comparison between in situ
9 evidence of human occupation and of climate change. This approach shows that the
10 timing of a prolonged drought at ca. 4400-3800 yr BP blankets the onset of cave
11 abandonment shortly after ca. 4403 cal yr BP, supporting the hypothesis that a climate
12 anomaly may have played a role in this cultural disruption.

1 **1 Introduction**

2 As drought in NW-Africa is a recurring phenomenon and prolonged dry conditions
3 exert a significant impact on local social systems, it becomes important to accurately
4 document the role of drought conditions on the area. For instance, the most recent
5 drought in Algeria began in 1998, as part of a widespread pattern of drying in the
6 N-Hemisphere, and brought considerable loss in regards to water resource and
7 agricultural yields (Hoerling and Kumar, 2003). Increasingly dry sub-tropical
8 conditions are predicted as one potential consequence of anthropogenic climate
9 change, but current general circulation models do not completely capture the
10 magnitude and spatial extent of observed drought conditions (Seager et al., 2007). To
11 help understand recent climate anomalies, paleoclimate studies are crucial to
12 characterize the range of potential natural variability in the past and to improve our
13 understanding of the links between regional drought and large scale forcing.
14 Instrumental data from weather stations in NW-Africa report less than one hundred
15 years. Tree ring based drought reconstructions in Algeria and Tunisia have been
16 extended back to the last nine centuries, which reveals large spatial heterogeneity of
17 past climate evolutions in NW-Africa and concludes that the climate anomaly
18 1998-2002 appears to be the most severe in the last millennium (Touchan et al., 2008;
19 Touchan et al., 2011). Holocene paleoclimate studies in other regions, however, have
20 suggested larger oscillations at centennial to millennial time scales highlighting the
21 need for new records from this area (Mayewski et al., 2004; Wanner et al., 2008).
22 A significant climate excursion ca. 4200 yr BP has been widely reported and is
23 considered as an ideal case to study the causes and effects of a large-scale climate
24 anomaly that occurred against background conditions similar to those of today
25 (Berkelhammer et al., 2013; Booth et al., 2005; Dixit et al., 2014; Roland, 2012). The
26 climatic expression of the 4200 yr BP event differs around the world. For example, it
27 has been documented as droughts in much of mid-to-low latitudes, across Africa, Asia
28 and N-America, wet and stormy in N-Europe and cooler in N-Atlantic (Booth et al.,

1 2005; Roland, 2012). More recently, this climatic anomaly was characterized by
2 extreme dry conditions on high-resolved speleothem isotope records from the Central
3 (Drysdale et al., 2006; Zanchetta et al., 2014) and E-Mediterranean basin
4 (Bar-Matthews and Ayalon, 2011), but, until now, such records have not available in
5 the W-Mediterranean which prevents us the correlation of past climate anomalies
6 across the basin.

7 Aside from its climatic interest, such an episode likely influenced numerous human
8 cultures. Major societal changes have been observed across the Mediterranean basin
9 during the Mid-Holocene, and in particular, a catastrophic desiccation ca. 4200 yr BP
10 has been suggested to trigger the collapse of the Akkadian Empire in Mesopotamia,
11 the Old Kingdom in Egypt and the Early Bronze Age civilizations of Greece and
12 Crete (Weiss and Bradley, 2000; Weiss et al., 1993; Wiener, 2014). These studies
13 have been stimulating an increasing number of debates on climate-culture relationship
14 (e.g., Coombes and Barber, 2005). Uncertainty regarding the societal impact of such
15 an event is still large, due in part that climatic evidence, in many cases, has been
16 derived from regions far from the distribution of ancient settlements (e.g., Cullen et
17 al., 2000). Although the 4200 yr BP dry event has been observed in several mid
18 latitude sites, the database remains incomplete and conflicting observations of
19 climatic conditions between seemingly adjacent regions exist (Magny et al., 2013;
20 Staubwasser and Weiss, 2006). Additionally, a recent study demonstrated that the
21 climatic impact on many agricultural settlements in ancient Near East was diverse
22 even within spatially limited cultural units (Riehla et al., 2014).

23 In N-Algeria, the extinction of large mammal species (e.g., *Syncerus antiquus*) during
24 the Mid-Holocene was correlated with regional climate aridity, likely due to the
25 competition with pastoralists and livestock for increasingly scarce water (Faith, 2014).
26 Similarly, the evidence of the aridity (i.e., the termination of the African Humid
27 Period) that provoked this extinction has been derived from the Sahara and its
28 surroundings (deMenocal et al., 2000), which is several hundred kilometres away,

1 leaving this assertion ambiguous and stimulating the search for new high resolution
2 paleoclimate records in the area.

3 In this study, we document the Mid-Holocene climate history in the Western
4 Mediterranean by decadal-resolved stable carbon and oxygen isotopes analyses of two
5 U/Th dated stalagmites from the Gueldaman GLD1 Cave of N-Algeria. We compare
6 the records with those established earlier in the Central and E-Mediterranean basin. In
7 addition, we describe archaeological deposits layers inside the cave whose ages have
8 been reasonably well constrained due to new radiocarbon dating. Finally we test the
9 links between cultural changes and climate anomalies with a particular emphasis on
10 the 4200 yr BP event.

11

12 **2 Samples and Methods**

13 **2.1. Study Site**

14 Gueldaman GLD1 Cave is one of a series of karstic caves formed within the SE-ward
15 slope of the Adrar Gueldaman ridge, western part of Babor mountains in N-Algeria
16 (Kherbouche et al., 2014). It is located close to the large Soummam River, 5-6 km
17 from the Akbou town, and approximately 65 km southern inland from the
18 W-Mediterranean Sea (36°26'N, 4°34'E, 507 m asl) (Fig. 1). Gueldaman GLD1 is a
19 relatively short cave (total extension of ~80 m) that developed in Jurassic limestone.
20 The entrance, facing to the SE, is a semi-circular ~6 m large arch, leading to a
21 dome-shaped ~10 m high and 6 m wide corridor which ends with the main chamber
22 “Grande Salle” at a depth of 30-40 m. Previous archaeological excavation and field
23 investigation suggest that Gueldaman GLD1 Cave has probably been open since at
24 least ca. 7 ka ago (Kherbouche et al., 2014). The area is covered by a thin layer (< 10
25 cm) of soil derived from the limestone bedrock, wind-blown silicate dust, and organic
26 matter from local vegetation such as *Pistacia lentiscus*, *Quercus ilex*, *Buxus*
27 *sempervirens*, typical Mediterranean *Garrigue* type plant assemblage (C3 dominated).

1 Local climate is Mediterranean semi-arid type, characterized by hot-dry summers and
2 mild-wetter winters. From the ERA-interim reanalysis data between 1979 and 2013
3 (<http://apps.ecmwf.int/datasets/>) the annual total rainfall is 516 mm, and the annual
4 mean temperature is 17.2 °C. Rainfall occurs rarely in the summer (37 mm) but
5 relatively evenly through the autumn (155 mm), winter (178 mm) and spring (147
6 mm). Gueldaman GLD1 Cave is well ventilated with the outside atmosphere due to its
7 larger opening and shorter extension. Hobo logger data at 10 min resolution from
8 November 2013 to April 2015 shows significant variations in cave temperature
9 ranging from 13.7 °C to 19.5 °C. The relative humidity varies from 56% to 94%.
10 Carbon dioxide has not been measured, but it is likely to be close to the atmospheric
11 value.

12 **2.2. Stalagmites Analyses**

13 Two stalagmites and three modern calcites samples were collected in 2012 and 2013
14 from the main chamber of Gueldaman GLD1 Cave. Both stalagmites were laid on the
15 cave floor during collection. Stalagmite GLD1-stm2 is 350 mm long and 100-200 mm
16 wide; stalagmite GLD1-stm4 is 203 mm long with a diameter of 50-120 mm (Fig. 2).
17 They were halved and polished along the longitudinal axis. It was noticed from the
18 sectioned sample that stalagmite GLD1-stm2 was broken at the depth of 5 mm/top
19 and covered by the calcite deposited at certain time after that point. The top 5 mm was
20 not analyzed in this study. Both stalagmites show well-marked laminae with several
21 shifts in the drip apex of the lower parts (Fig. 2). Black bandings, with visible
22 incorporations of charcoal particles, are found throughout both stalagmite profiles.

23 **U/Th dating** - Seventeen powder samples were drilled from the two stalagmites and
24 dated by a multi-collector inductively coupled plasma mass spectrometer. The
25 procedure to separate uranium and thorium were referred to Edwards et al. (1987) and
26 Cheng et al. (2013). The dating work was carried out at the University of Minnesota
27 (USA) and the Xi'an Jiaotong University (China). One dating from the base part of

1 stalagmite GLD1-stm2, for the exploration of preliminary age frame, was done at the
2 Laboratoire des Sciences du Climat et de l'Environnement (LSCE, France). The U/Th
3 dates were reported in years before 2000 AD. (Fig. 2, Table 1). The age model for
4 both stalagmites was developed using the StalAge program (Scholz and Hoffmann,
5 2011) where a linear interpolation between depth and age is made through each
6 progressive triplet of adjacent U/Th dates (Fig. 3). This procedure provides a
7 quantitative estimate of age uncertainty continuously along the record despite having
8 analytical constraints only at locations where the U/Th dates exist. Stalagmite growth
9 rates were calculated based on the StalAge age model (Fig. 4).

10 **Stable isotopes** - Four hundred and thirty samples were drilled every 1 to 2 mm along
11 the stalagmite central growth axis (Fig. 2). Stable carbon and oxygen isotopes
12 compositions of both stalagmites and modern calcites were measured using a
13 VG-OPTIMA mass spectrometer at the LSCE. For each analysis, 60 to 80 μg calcite
14 powder is reacted with phosphoric acid at 90 °C, and the resultant CO_2 is measured
15 relative to a reference gas that has been calibrated against a series of isotopic
16 standards. Duplicates were run every 10 to 20 samples to check replicability. All
17 values are reported in ‰ relative to the V-PDB (Fig. 4). The error is 0.08‰ for $\delta^{18}\text{O}$
18 and 0.05 ‰ for $\delta^{13}\text{C}$.

19 **2.3. Archaeological analyses**

20 Archaeological excavations were carried out at two sectors S2 and S3 inside the
21 Gueldaman GLD1 Cave during the 2010-2012 campaign (Fig. 1). This work consisted
22 mainly in collecting, identifying, and referencing the archaeological materials found
23 in stratigraphic layers (refer to Kherbouche et al. (2014) for details). More than 7000
24 anthropogenic remains were collected, consisting mainly of faunal remains, ceramic,
25 and lithic and bone tools. Besides, all sediments were water screened through 1.5 mm
26 and 4 mm mesh and subjected systematically to flotation with collection in a 250 μm
27 mesh yielding a huge amount of charcoals. Initial radiocarbon dating of upper

1 stratigraphic sequences from S2 and S3 gave the median ages ranging from ca. 6800
2 to 1500 cal yr BP (Kherbouche et al., 2014). In order to refine the chronology of these
3 deposits, in this study, six new charcoal samples were collected from the key
4 archaeological layers in excavation area MN 47/48 of S2. These samples were dated
5 using the AMS radiocarbon method at the CEA Saclay (France). Detailed procedures
6 of the chemical preparation and the dating in the lab were referred to Cottreau et al.
7 (2007). The dates were calibrated using the IntCal13 dataset (Reimer et al., 2013) and
8 reported in years before 2000 AD (Table 2).

9

10 **3 Results**

11 **3.1. Stalagmites U/Th dates and growth rates**

12 The uranium contents of measured stalagmites samples are relatively high ranging
13 from 95 to 225 ppb (Table 1). The 2 sigma U/Th errors vary from 20 to 210 years with
14 an average of 77 years (1.6%). The U/Th date (5070 ± 194 yr BP) of sample
15 GLD1-stm4-47 was detected as a major outlier by the StalAge program, thus, it was
16 not used to calculate the final age model. Calculated StalAge age model for stalagmite
17 GLD1-stm4 shows large errors up to 500 years during ca. 4900-4200 yr BP (Fig. 3).
18 This may partly be due to relatively large errors of adjacent U-series dates and/or
19 inappropriate hypotheses applied in the algorithm. Based on individual StalAge age
20 model, stalagmite GLD1-stm2 grew from ca. 6200 to 4000 yr BP (4100 yr BP if
21 excluding the top 5 mm), whereas stalagmite GLD1-stm4 grew from ca. 5800 to 3200
22 yr BP (Fig. 3).

23 Stalagmite GLD1-stm2 shows high and variable growth rates (mean = $180 \mu\text{m yr}^{-1}$)
24 with higher values $\sim 400 \mu\text{m yr}^{-1}$ at ca. 4800-4600 yr BP; whereas stalagmite
25 GLD1-stm4 shows relatively lower and less variable growth rates (mean = $120 \mu\text{m yr}^{-1}$)
26 with higher values $\sim 200 \mu\text{m yr}^{-1}$ at ca. 3800-3200 yr BP (Fig. 4).

1 **3.2. Stable carbon and oxygen isotopes**

2 The isotopic compositions of modern calcite vary from $-5.40\text{\textperthousand}$ to $-5.56\text{\textperthousand}$ for the
3 $\delta^{18}\text{O}$ and from $-8.43\text{\textperthousand}$ to $-10.34\text{\textperthousand}$ for the $\delta^{13}\text{C}$. The $\delta^{18}\text{O}$ values from stalagmites
4 GLD1-stm2 and GLD1-stm4 range from $-7.8\text{\textperthousand}$ to $-2.8\text{\textperthousand}$ and from $-7.3\text{\textperthousand}$ to $-0.6\text{\textperthousand}$,
5 respectively; the $\delta^{13}\text{C}$ values range from $-10.6\text{\textperthousand}$ to $-3.3\text{\textperthousand}$ and from $-11.9\text{\textperthousand}$ to $-0.6\text{\textperthousand}$,
6 respectively. The $\delta^{18}\text{O}$ and $\delta^{13}\text{C}$ significantly correlate in both stalagmites: $R = 0.87$, $P < 0.01$ for GLD1-stm2 and $R = 0.92$, $P < 0.01$ for GLD1-stm4. Albeit the different
7 amplitudes, the isotopic profiles of the two stalagmites show similarities during their
8 common development of ca. 5800-4000 yr BP: relatively elevated isotope values are
9 found at ca. 5700-5400 yr BP, ca. 5200 yr BP, and ca. 4500 yr BP (Fig. 4). Two other
10 isotopically enriched periods in stalagmite GLD-stm2 are found at ca. 6200 yr BP and
11 ca. 4900 yr BP (Fig. 4). There is a common isotopic enrichment trend since ca.
12 4800-4600 yr BP (depending on individual age model; abrupt in stalagmite
13 GLD1-stm4 whereas more gradual in GLD1-stm2). Toward the end of this trend, the
14 most prominent anomaly occurs in stalagmite GLD1-stm4 at ca. 4400-3800 yr BP
15 during which the $\delta^{18}\text{O}$ values are enriched by approximately $3.5\text{\textperthousand}$ relative to the
16 background values of that time as well as the modern calcite values for a period of
17 ~ 500 years (Fig. 4). Specifically within this anomalous period, there is a mild isotopic
18 depletion at ca. 4200-4000 yr BP, blanketed by two significant enrichments at ca.
19 4400-4200 yr BP and ca. 4000-3800 yr BP (Fig. 4). The last part, ca. 3800-3200 yr BP,
20 of GLD1-stm4, is characterized by a $\delta^{18}\text{O}$ recovery of about $-3\text{\textperthousand}$, synchronous with
21 increased growth rates (Fig. 4).

23 **3.3. Anthropogenic deposits and ^{14}C dates**

24 Excavations inside Gueldaman GLD1 Cave revealed a large variety of archeological
25 remains and, among them, are numerous precious macro charcoals that have been
26 used for establishing the chronology of the deposits. In the $\sim 7 \text{ m}^2$ total excavated area
27 of S2, more than 7000 archaeological objects were identified and consisted of faunal

1 remains, lithic artifacts and grinding equipment, potteries, bone tools, ornaments, and
2 ochre. In addition, a fragment of a human mandible and two isolated teeth were found
3 during the excavation 2010-2012 in Gueldaman GLD1 Cave (Kherbouche et al.,
4 2014). These deposits belong mainly to the Neolithic; only the top level of the
5 sequence contains potsherds of the historic period. In the lower Neolithic levels,
6 identified domestic species (i.e. sheep and goats) represented ~25% of total faunal
7 assemblages ($N = 2378$) suggesting a partly pastoral based economy. The potteries (N
8 = 825) are mostly related to cooking vessels of 25-40 cm rim diameter. Hundreds of
9 black charcoals (>1 cm) were found and always associated with ceramic
10 concentrations suggesting evidence of cooking activities.

11 Determined radiocarbon dates give the median ages of the sequence between 7002
12 and 1482 cal yr BP, with their 2σ -error intervals varying from 132 to 374 years (Table
13 2). These dates provide a first chronology for the archaeological deposits excavated
14 from sector S2 (Fig. 6) (Kherbouche et al., 2014): anthropogenic remains (i.e.
15 charcoals, bones, teeth and potteries) are numerous during ca. 7002-6003 cal yr BP
16 (depths of ~150-120 cm), decreased at ca. 6003-4918 cal yr BP (depths of ~120-105
17 cm), most abundant in the period of ca. 4918-4403 cal yr BP (depths of 105-75 cm),
18 significantly diminished during the long interval of ca. 4403-1484 cal yr BP (depths
19 of 75-60 cm), and finally, numerous again from ca. 1484 cal yr BP (depths of ~60-50
20 cm). With an overall decrease in archeological materials, there are two levels clearly
21 marked by their poverty in charcoal and pottery during the periods of ca. 6003-4918
22 cal yr BP and ca. 4403-1484 cal yr BP (Fig. 6).

23

24 **4 Discussions**

25 **4.1. Climatic significance of stalagmites proxies**

26 Under isotopic equilibrium precipitation, stalagmite calcite $\delta^{18}\text{O}$ depends mainly on
27 the temperature of calcite-water fractionation and on the $\delta^{18}\text{O}$ of drip water that is

1 controlled by local rainfall $\delta^{18}\text{O}$ (Genty et al., 2014; Lachniet, 2009). Observations
2 from the IAEA network show that the rainfall $\delta^{18}\text{O}$ at many Mediterranean stations
3 (including one in Algiers, Algeria) are partly controlled by the amount of rainfall
4 (IAEA, 2005), which is coherent with previous studies that stalagmite $\delta^{18}\text{O}$ records
5 from the Mediterranean regions were interpreted to primarily reflect changes in
6 rainfall amount (inversely correlated) (e.g., Bar-Matthews and Ayalon, 2011;
7 Bar-Matthews et al., 2003; Bar-Matthews et al., 1997; Drysdale et al., 2006;
8 Drysdalea et al., 2004; Zanchetta et al., 2014). Therefore, higher stalagmite $\delta^{18}\text{O}$
9 values are expected during periods of decrease in rainfall (drier). The temperature
10 effect on calcite-water fractionation, on the other hand, is partly counteracted by the
11 condensation temperature effect on rainfall $\delta^{18}\text{O}$ (Drysdale et al., 2006). We notice
12 that this interpretation may particularly hold true for the present study because the
13 regional temperature seems to has been relatively constant since the Mid-Holocene
14 (Martrat et al., 2004).

15 Stalagmite $\delta^{13}\text{C}$ variations have several potential causes, the most likely, considering
16 the studied location and time interval, being variations in soil CO_2 input and water
17 flow rate (Genty et al., 2001a; McDermott, 2004). Despite the fact that soil biogenic
18 CO_2 production varies according to both temperature and moisture level, moisture is
19 likely to be a major controlling factor due to low temperature variability of the
20 considered time interval and limited water availability under semiarid climates.
21 Moisture also influences water flow rate and thus the CO_2 loss during the prior calcite
22 precipitation (Fairchild et al., 2000). Longer residence time due to lower flow rate,
23 under diminished moisture condition, enhances CO_2 loss and preferential ^{12}C removal
24 from solution causing enrichments in stalagmite $\delta^{13}\text{C}$ (Johnson et al., 2006; Mickler et
25 al., 2004). Eventually, atmospheric rainfall largely determines the moisture level and
26 controls the $\delta^{13}\text{C}$ variations. Therefore, the significant correlation of stalagmite $\delta^{13}\text{C}$
27 and $\delta^{18}\text{O}$ may suggest a common control of rainfall.

28 The rainfall signal imprinted in the Gueldaman stalagmite isotopes (inversely

1 correlated) is probably amplified by two other processes - evaporation and
2 disequilibrium isotopic fractionation (Mickler, 2006) that are very likely to have
3 occurred at the Gueldaman GLD1 Cave due to its large entrance. Longer residence
4 time during drier (lower rainfall) periods would allow extended evaporative and
5 non-equilibrium fractionations, which drives stalagmite isotopes further higher
6 (Mickler et al., 2004). It has recently been observed that evaporation in semiarid caves
7 could cause 4-5‰ $\delta^{18}\text{O}$ enrichments of a wide range of drip waters (Cuthbert et al.,
8 2014). The Hendy test (i.e. studying the isotopic variation in contemporaneous
9 laminae (Hendy, 1971)) carried out at three different depths in stalagmite GLD1-stm2
10 show that the $\delta^{18}\text{O}$ and $\delta^{13}\text{C}$ significantly correlate and simultaneously increase by up
11 to ~1‰ from the apex to the edge probably due to the presence of progressive kinetic
12 fractionations when feeding waters flow outwards from the apex, suggesting that the
13 stalagmite formed out of isotopic equilibrium (Supplement). These two processes may
14 partly account for the significant correlation of the $\delta^{18}\text{O}$ and $\delta^{13}\text{C}$ profiles in both
15 stalagmites ($R=0.87$ for GLD-stm2; $R=0.92$ for GLD1-stm4). Comparisons of two
16 stalagmites show different amplitudes in their isotopic profiles. This might be due to:
17 1) having been fed by reservoirs that smooth rainfall signal differently, and 2) having
18 been suffered from variable evaporative and kinetic enrichments associated with
19 different recharge features. Albeit this discrepancy the isotopic profiles of two
20 stalagmites broadly show similar patterns. Consequently, synchronous $\delta^{18}\text{O}$ and $\delta^{13}\text{C}$
21 variations in the two stalagmites can be interpreted in terms of humidity change. A
22 prolonged severe drought is inferred from the most elevated isotopes values during ca.
23 4400-3800 yr BP together with drier periods from higher values at ca. 6200 yr BP, ca.
24 5700-5400 yr BP, ca. 5200 yr BP, and ca. 4500 yr BP (Fig. 4), while wetter periods are
25 suggested from depleted isotopes at ca. 4600-5100 yr BP and ca. 5300 yr BP.
26 Moreover, stalagmite growth phase has long been regarded as an environmental
27 indicator (e.g., Genty et al., 2001b; Stoll et al., 2013) and could be used to
28 complement and/or test the climatic interpretation from isotope records. Water

1 availability is an essential factor for stalagmite growth in arid-to-semiarid areas, as
2 shown by Vaks et al. (2013) who correlated growth periods well with periods of
3 effective rainfall regimes. The growth cessation of stalagmite GLD1-stm2 at ca. 4000
4 yr BP may suggest a phase of increased aridity, which is consistent with the dryness
5 inferred from elevated isotopes (Fig. 4). However, the continuous growth of
6 stalagmite GLD1-stm4 at that time suggests that the growth cessation might also have
7 been caused by shifts in dripping position under deteriorating climates (Fairchild and
8 Baker, 2012). Moreover, fast stalagmite growths together with wide diameters usually
9 are associated with high drip rates suggesting humid conditions. A wet period ca.
10 4800-4600 yr BP is indicated by the high growth rates of stalagmite GLD1-stm2,
11 which is broadly in line with the humid period inferred from depleted isotopes (Fig. 4).
12 Another wetter period ca. 3800-3200 yr BP is suggested by faster growths and
13 relatively depleted isotopes of stalagmite GLD1-stm4 (Fig. 4). The discrepancy in the
14 growth rate profiles of the two stalagmites is possibly due in part to 1) the lack of
15 substantial U/Th dating especially for stalagmite GLD1-stm4 between 5023 and 4197
16 yr BP, and/or 2) site-specific processes due to different reservoirs play a key role in
17 controlling stalagmite growth.

18 Finally, the modern calcite isotopic values fall in the range of two stalagmite records
19 (Fig. 4), which suggests that the current humidity condition in N-Algeria seems to be
20 within the range of its Mid-Holocene variability. The average $\delta^{18}\text{O}$ value during ca.
21 4400-3800 yr BP in stalagmite GLD1-stm4 is more enriched by about 3.5‰ relative
22 to the modern values (Fig. 4), therefore, the 4400-3800 yr BP climate anomaly may be
23 considered analogous to end numbers of the most recent and ongoing drying.

24 **4.2. Mid-Holocene climate anomalies across the Mediterranean basin
25 and their dynamic implications**

26 High-resolution absolute-dated Mid-Holocene climate records are rare in the
27 W-Mediterranean basin, however, there are number of paleoenvironment studies using

1 sediment cores that document large oscillations in vegetation ecology and provide
2 clues of climate change during the Mid-Holocene. A drying trend from ca. 4600 cal yr
3 BP onwards was inferred, based on the decreasing pollen ratio of deciduous
4 broad-leaf *versus* evergreen sclerophyllous taxa at Capestang in the Mediterranean
5 S-France (Jalut et al., 2000). At a nearby site in NE-Spain, the most arid
6 Mid-Holocene condition at ca. 4800-4000 cal yr BP was interpreted using maximum
7 salinity values, more positive organic carbon isotope values, and decreased algal
8 productivity in Estanya Lake (Morrellon et al., 2009). In the Mediterranean S-Spain,
9 desertification phases at ca. 5200 cal yr BP and ca. 4100 cal yr BP were inferred using
10 multiple palaeoecological indicators including pollen, microcharcoal, spores of
11 terrestrial plants, fungi, non-siliceous algae, and other microfossils in Siles Lake
12 (Carrión, 2002). Similar environment changes have also been observed in the Central
13 Mediterranean basin, as shown by a synthesis study of lacustrine palynological data
14 which suggested a dryness peaking at ca. 4000 cal yr BP (Sadari et al., 2011).
15 Evaluated carbonate oxygen isotopes from Lake Shkodra were argued to be an
16 indicator of dryness at ca. 4100-4000 cal yr BP (Zanchetta et al., 2012b). Increasing
17 aridity at ca. 5000-4000 cal yr BP was suggested to explain the increases in non-tree
18 pollen percentage and micro charcoal content in the Lago di Pergusa Lake, Sicily
19 (Roberts et al., 2011; Sadari and Giardini, 2007; Sadari and Narcisi, 2001). Closer to
20 our site, a study at Preola Lake, E-Sicily, documented a significant low stand lake
21 level at ca. 4500-4000 cal yr BP suggesting extreme aridity (Magny et al., 2011).
22 Moreover, six tephra layers were carefully studied to correlate climate anomalies at ca.
23 4500-3800 cal yr BP from different archives in central Mediterranean (Zanchetta et al.,
24 2012a). In the east, Finné et al. (2011) reviewed the climate history of
25 E-Mediterranean over the last 6000 years and concluded with much evidence of
26 drying conditions at ca. 4600-3800 yr BP. Although the sampling and dating
27 resolutions in most of the above studies are low, they are in good agreement with the
28 present study regarding the 5200 yr BP dry event, the drying trend from 4800-4600 yr

1 BP onward, and the 4400-3800 yr BP drought.

2 Recently, high frequency Mid-Holocene climate change has been well documented by

3 multiple detailed speleothem studies from the Central and E-Mediterranean basin (Fig.

4 5). Drysdale et al. (2006) demonstrated a severe drought peaked at 4400-3800 yr BP

5 through multiproxy analyses on a U/Th-dated flowstone from Renella Cave, Central

6 Italy. This finding is supported by following work at nearby Corchia Cave. Zanchetta

7 et al. (2007) established a high resolution speleothem isotope record for the entire

8 Holocene and interpreted it as an indicator of rainfall change, in which a drier period

9 persisting from ca. 4800 to 3800 yr BP could be inferred from relatively elevated $\delta^{18}\text{O}$

10 values. Elemental analysis on the same stalagmite by Regattieri et al. (2014) presented

11 more clear signals of dryness peaked at ca. 4700-4200 yr BP. In the E-Mediterranean

12 basin, Bar-Matthews and Ayalon (2011) explicitly discussed the Mid-Holocene

13 climate change by high resolution dating and isotopic analyses on speleothems from

14 Soreq Cave in Israel; they identified multiple dry events at 6250-6180 yr BP,

15 5700-5600 yr BP and 5250-5170 yr BP as well as a long drying trend since ca. 4700

16 yr BP peaked at 4200-4050 yr BP. Zanchetta et al. (2014) carefully compared the

17 speleothem isotope records from Corchia Cave and Soreq Cave in Central and

18 E-Mediterranean basin, and found two coeval dry events at ca. 5600 yr BP and ca.

19 5200 yr BP from the comparable $\delta^{18}\text{O}$ enrichments in two speleothems. Detailed

20 comparisons of these speleothem records with our new records from Gueldaman

21 GLD1 Cave reveal many consistencies. In particular, periods with elevated $\delta^{18}\text{O}$

22 values at ca. 5700-5400 yr BP, 5200 yr BP and 4400-3800 yr BP observed in

23 Gueldaman stalagmites are all identifiable in the speleothems from Corchia, Renella

24 and Soreq Cave (Fig. 5), suggesting that anomalous dryness at these periods

25 synchronously developed across the Mediterranean basin. These observations indicate

26 that climates in the Mediterranean basin might have been under an identical regional

27 scale atmospheric regime during the Mid-Holocene.

1 It has been suggested that climate change in mid-latitude Europe and Mediterranean
2 might arise from a perturbation of the Westerlies from a high-latitude trigger (i.e. the
3 North Atlantic) (Bond et al., 2001; Drysdale et al., 2006; Zanchetta et al., 2014) or
4 from dynamics within the tropics (Booth et al., 2005; Hoerling and Kumar, 2003).
5 The three dry periods in the Mediterranean are broadly in phase with the ice rafting
6 events in the subpolar North Atlantic (Bond et al., 2001), which suggests some links
7 with the N-Atlantic circulation. Based on the coincidence with the elevated wind
8 strength in Iceland (Jackson et al., 2005), Zanchetta et al. (2014) argued that the dry
9 events at ca. 5700-5400 and ca. 5200 yr BP might be caused by reduction of vapor
10 advection into the Mediterranean, due to the intensification and northward
11 displacement of the N-Atlantic Westerlies. However, lacking evidence of strengthened
12 wind in the fourth millennium BP argues for a different forcing of the 4400-3800 yr
13 BP drought. The considerably lower amplitude of the Bond ice rafting event at ca.
14 4200 yr BP than at the fifth millennium BP also indicates a varied ocean-atmosphere
15 circulation state. The modern mid-latitude droughts (1998-2002) have been linked to
16 the increased warmth in equatorial oceans (Booth et al., 2005). During this event, SST
17 changes lead to persistent high pressure over the Northern Hemisphere's mid-latitudes,
18 causing widespread synchronous drought (Hoerling and Kumar, 2003). However, the
19 challenge in applying the dynamics under the 1988-2002 drought towards an
20 understanding of the 4400-3800 yr BP climate anomaly is that while the mechanism
21 operate effectively on short time scales, it has never been tested as to whether they
22 could produce an anomalous climate mode for several centuries (Berkelhammer et al.,
23 2013). General circulation model simulations that begin with realistic boundary
24 conditions and are perturbed with a variety of forcings have been successfully
25 undertaken to understand potential mechanisms that lead to the 8200 yr BP event
26 (Tindall and Valdes, 2011). Similar efforts would be a useful starting point to produce
27 hypotheses for the dynamical underpinnings of the 4200 yr BP event.

4.3. Possible relations between climate anomaly and cultural change

A regional drought ca. 4200 yr BP has been widely linked to ancient cultural changes in the E-Mediterranean and the Asia (Staubwasser and Weiss, 2006), though, in many cases, climatic inferences have been derived from sites that are distant to these human settlements. For instance, evidence of reduced precipitation from elevated $\delta^{18}\text{O}$ of Soreq stalagmites (Israel) and increased dust input into the Gulf of Oman sediment core has been suggested to contribute to the collapse of the Akkadian imperial in Mesopotamia (Bar-Matthews and Ayalon, 2011; Cullen et al., 2000; Weiss et al., 1993). Similarly, a dry period inferred from reduced discharge of the Indus river and elevated $\delta^{18}\text{O}$ of a NE-Indian stalagmite has been linked with the Indus Valley de-urbanization (Berkelhammer et al., 2013; Staubwasser et al., 2003; Staubwasser and Weiss, 2006). A recent study in ancient Near East, however, revealed that the regional impact of the drought on ancient civilizations, being influenced by geographic factors and human technology, were highly diverse even within spatially limited cultural units (Riehla et al., 2014). This highlights the need for caution when linking evidence of human activities from a site to evidence of climate oscillations from another one.

The present study in the Gueldaman GLD1 Cave provides an opportunity to test climate-culture relations by comparing in situ archeological sequences and high resolution paleoclimate records, thereby avoiding the uncertainty of inter-site correlation arising from complex spatial heterogeneity in climate and demography.

To facilitate the comparison, stalagmite-inferred climate changes at the cave site during ca. 6200-3200 yr BP are separated into four periods 1-4 (Table 3):

- Period 1 (~6200-5100 yr BP): wet, superimposed by several centennial-scale drier events;
- Period 2 (~5100-4400 yr BP): wettest, ending with a ~200-yr-long shift from the wettest to extreme dry conditions;

1 - Period 3 (~4400-3800 yr BP): a drought-like climatic anomaly;
2 - Period 4 (~3800-3200 yr BP): relatively wetter.

3 In parallel, from the abundance of archaeological remains (especially bone, charcoal
4 and pottery) (Fig. 6), the temporal evolution of past cave occupations can be separated
5 into five phases 0-4 (Table 3):

6 - Phase 0 (~7002-6003 cal yr BP): permanent and intensive occupation;
7 - Phase 1 (~6003-4918 cal yr BP): permanent but less intensive occupation;
8 - Phase 2 (~4918-4403 cal yr BP): permanent and most intensive occupation;
9 - Phase 3 (~4403-1484 cal yr BP): abandonment of the cave/occasional visits;
10 - Phase 4 (~1484 cal yr BP-): re-occupation of the cave.

11 Correlations can be identified when comparing the climatic and archaeological
12 records, though this does not necessarily mean that occupation of the cave depends
13 merely on climate (Table 3; Fig. 7). When the climate was wet and variable ca.
14 6200-5100 yr BP (Period 1), the Gueldaman GLD1 Cave preserved a few bones and
15 rare charcoals and potteries (Phase 1) (Fig. 7). When the climate was wettest ca.
16 5100-4400 yr BP (Period 2), the most abundance of bones, charcoals and potteries
17 suggests a permanent and more intensive occupation of the cave (Phase 2) (Fig. 7).
18 More striking is the drought-like climate anomaly that has been establishing ca.
19 4400-3800 yr BP (Period 3), from which the cave was abandoned for ca. 3000 years
20 (indicated by a dramatic decrease in anthropogenic remains, especially charcoal and
21 pottery) (Phase 3) (Fig. 7). The rarer bones seen in this period imply that the cave
22 might have been occasionally visited until its re-occupation at ca. 1484 cal yr BP (Fig.
23 7). These observations argue for links between climate and settlement activity
24 especially during the 4200 yr BP climate anomaly. Water availability was likely
25 crucial to maintain the Neolithic community at Gueldaman, N-Algeria and the
26 prolonged severe drought ca. 4400-3800 yr BP might have played a role in triggering
27 the settlement abandonment, indicating that the pastoral economy may not be as
28 resistant, as commonly assumed, to climate anomaly in semiarid area.

1 Moreover, the sole piece of the bone from large ungulate (supposed to be elephant or
2 rhinoceros) found at the depth of ~110 cm (Kherbouche et al., 2014) was anchored by
3 two calibrated ¹⁴C dates from present study between 6003 and 4913 cal yr BP, which
4 is in line with the latest survival of large mammal species (e.g., *S. antiquus*) at the
5 proximate sites of N-Algeria during the Mid-Holocene (Faith, 2014 and references
6 wherein). The extinction of the Mid-Holocene large mammal in N-Algeria was
7 attributed to the competition with pastoralists and livestock for increasingly scarce
8 water, corresponding with an abrupt climatic shift toward extreme aridity in the
9 Sahara region ca. 5500 cal yr BP (i.e. the end of the Humid Africa Period (deMenocal
10 et al., 2000) (Faith, 2014). Recently, the timing of this climatic transition was refined
11 to ca. 4900 yr BP ± 200 yrs (McGee et al., 2013). In addition, a paleoenvironmental
12 study in the Sahara revealed that the Mid-Holocene deteriorations of terrestrial
13 ecosystem and climate culminated at ca. 4200-3900 cal yr BP (e.g., Kröpelin et al.,
14 2006). Therefore, it is more likely based on evidence from the Gueldaman GLD1
15 Cave and the proximate sites (Faith, 2014) that extinction of large mammal/ungulate
16 in N-Algeria occurred during the prolonged drought ca. 4400-3800 yr BP.

17

18 **5 Conclusions**

19 It is increasingly clear based on a growing number of records spanning across much
20 of mid-to-low latitudes, N-Europe, and the Atlantic ocean that there was a significant
21 large scale climate anomaly at around 4200 yr BP (Booth et al., 2005). The 4200 yr
22 BP aridity that had been suggested to affect the Early Bronze Age populations from
23 the Aegean to ancient Near East was recently characterized by high-resolution
24 speleothem records from the Central and E-Mediterranean basin (Bar-Matthews and
25 Ayalon, 2011; Drysdale et al., 2006; Zanchetta et al., 2014). The new record presented
26 here from the Gueldaman GLD1 Cave in N-Algeria provides increased evidence of a
27 prolonged severe drought ca. 4400-3800 yr BP, which suggests that the Mid-Holocene
28 dryness spread to the W-Mediterranean of N-Africa.

1 Radiocarbon dating made on charcoals constrains reasonably well the age of
2 archaeological deposits excavated inside the cave (Kherbouche et al., 2014) and
3 reveals significant changes in human occupation during the last ca. 7000 years.
4 Comparison of the stalagmite record with in situ archaeological sequence suggests
5 synchronicity between climate and settlement activity. Relatively wet/dry periods
6 coincide with the periods of more/less intensive human occupation. Particularly, the
7 timing of the prolonged drought at ca. 4400-3800 yr BP blanket the onset of the cave
8 abandonment event shortly after ca. 4403 cal yr BP, which argues a possible role of
9 climate anomaly in this societal disruption. Further work on pollen-based
10 reconstruction of vegetation/environment change from the excavation sequence and
11 on refinement of the chronology of transitions between different occupation phases
12 would potentially uncover the intrinsic relations among climate, environment and
13 settlement. It is suggested that the methodology and the findings from the present
14 study at the Gueldaman GLD1 Cave be applied and tested at other sites.
15

16 **Acknowledgements**

17 Radiocarbon dating were analysed by Jean-Pierre Dumoulin at ARTEMIS (LMC14,
18 Saclay). We thank Edwige Pons-Branchu, Monique Pierre for the U/Th dating of the
19 base part of stalagmite GLD1-stm2 during the earlier stage of this study. We also
20 thank Lijuan Sha at the Xi'an Jiaotong University for assistance with the U/Th dating.
21 We appreciate Russell N. Drysdale, Giuliano Zanchetta and Miryam Bar-Matthews
22 for sharing the isotopic data shown in Figure 6. Thanks to Cecilia Garrec for editing
23 assistance. We are thankful to Giuliano Zanchetta and an anonymous referee for their
24 constructive comments which improved this paper. This work was funded by the
25 CNRS INSU program PALEOMEX-ISOMEX, the NSFC grant 41230524 and the
26 CSC scholarship.
27

28 **References**

1 Bar-Matthews, M. and Ayalon, A.: Mid-Holocene climate variations revealed by
2 high-resolution speleothem records from Soreq Cave, Israel and their correlation with
3 cultural changes, *Holocene*, 21, 163-171, 2011.

4 Bar-Matthews, M., Ayalon, A., Gilmour, M., Matthews, A., and Hawkesworth, C. J.:
5 Sea-land oxygen isotopic relationships from planktonic foraminifera and speleothems
6 in the Eastern Mediterranean region and their implication for paleorainfall during
7 interglacial intervals, *Geochim. Cosmochim. Acta*, 67, 3181-3199, 2003.

8 Bar-Matthews, M., Ayalon, A., and Kaufman, A.: Late Quaternary Paleoclimate in the
9 Eastern Mediterranean Region from Stable Isotope Analysis of Speleothems at Soreq
10 Cave, Israel, *Quat. Res.*, 47, 155-168, 1997.

11 Berkelhammer, M., Sinha, A., Stott, L., Cheng, H., Pausata, F. S. R., and Yoshimura,
12 K.: An abrupt shift in the Indian Monsoon 4000 years ago. In: *Climates, Landscapes,
13 and Civilizations*, Giosan, L., Fuller, D. Q., Nicoll, K., Flad, R. K., and Clift, P. D.
14 (Eds.), American Geophysical Union, Washington, DC, 75-87, 2013.

15 Bond, G., Kromer, B., Beer, J., Muscheler, R., Evans, M. N., Showers, W., Hoffmann,
16 S., Lotti-Bond, R., Hajdas, I., and Bonani, G.: Persistent Solar Influence on North
17 Atlantic Climate During the Holocene, *Science*, 294, 2130-2136, 2001.

18 Booth, R. K., Jackson, S. T., Forman, S. L., Kutzbach, J. E., E.A. Bettis, I., Kreig, J.,
19 and Wright, D. K.: A severe centennial-scale drought in midcontinental North
20 America 4200 years ago and apparent global linkages, *The Holocene*, 15, 321 - 328,
21 2005.

22 Carrión, J. S.: Patterns and processes of Late Quaternary environmental change in a
23 montane region of southwestern Europe, *Quat. Sci. Rev.*, 21, 2047-2066, 2002.

24 Cheng, H., Edwards, L. R., Shen, C. C., Polyak, V. J., Asmerom, Y., Woodhead, J.,
25 Hellstrom, J., Wang, Y., Kong, X., Späl, C., Wang, X., and Alexander Jr, E. C.:

1 Improvements in ^{230}Th dating, ^{230}Th and ^{234}U half-life values, and U-Th isotopic
2 measurements by multi-collector inductively coupled plasma mass spectrometry,
3 *Earth Planet. Sci. Lett.*, 371-372, 82-91, 2013.

4 Coombes, P. and Barber, K.: Environmental determinism in Holocene research:
5 causality or coincidence?, *Area*, 37, 303-311, 2005.

6 Cottreau, E., Arnold, M., Moreau, C., Baque, D., Bavay, D., Caffy, I., Comby, C.,
7 Dumoulin, J.-P., Hain, S., Perron, M., Salomon, J., and Setti, V.: Artemis, the New
8 ^{14}C AMS14 in Saclay, France, *Radiocarbon*, 49, 291-299, 2007.

9 Cullen, H. M., deMenocal, P. B., Hemming, S., Hemming, G., Brown, F. H.,
10 Guilderson, T., and Sirocko, F.: Climate change and the collapse of the Akkadian
11 empire: Evidence from the deep sea, *Geology*, 28, 379-382, 2000.

12 Cuthbert, M. O., Baker, A., Jex, C. N., Graham, P. W., Treble, P. C., Andersen, M. S.,
13 and Acworth, R. I.: Drip water isotopes in semi-arid karst: Implications for
14 speleothem paleoclimatology, *Earth Planet. Sci. Lett.*, 395, 194-204, 2014.

15 deMenocal, P., Ortiz, J., Guilderson, T., Adkins, J., Sarnthein, M., Baker, L., and
16 Yarusinsky, M.: Abrupt onset and termination of the African Humid Period: rapid
17 climate responses to gradual insolation forcing, *Quat. Sci. Rev.*, 19, 347-361, 2000.

18 Dixit, Y., Hodell, D. A., and Petrie, C. A.: Abrupt weakening of the summer monsoon
19 in northwest India ~4100 yr ago, *Geology*, 42, 339-342, 2014.

20 Drysdale, R., Zanchetta, G., Hellstrom, J., Maas, R., Fallick, A., Pickett, M.,
21 Cartwright, I., and Piccini, L.: Late Holocene drought responsible for the collapse of
22 Old World civilizations is recorded in an Italian cave flowstone., *Geology*, 34,
23 101-104, 2006.

24 Drysdalea, R. N., Zanchetta, G., Hellstrom, J. C., Fallick, A. E., Zhao, J.-x., Isola, I.,

1 and Bruschi, G.: Palaeoclimatic implications of the growth history and stable isotope
2 ($\delta^{18}\text{O}$ and $\delta^{13}\text{C}$) geochemistry of a Middle to Late Pleistocene stalagmite from
3 central-western Italy, *Earth Planet. Sci. Lett.*, 227, 215- 229, 2004.

4 Edwards, R. L., Chen, J. H., and Wasserburg, G. J.: ^{238}U - ^{234}U - ^{230}Th - ^{232}Th systematics
5 and the precise measurements of time over the past 500000 years., *Earth Planet. Sci.*
6 *Lett.*, 81, 175-192, 1987.

7 Fairchild, I. J. and Baker, A.: *Speleothem science - from process to past environments.*
8 John Wiley & Sons, Ltd, Chichester, UK, 2012.

9 Fairchild, I. J., Borsato, A., Tooth, A. F., Frisia, S., Hawkesworth, C. J., Huang, Y. M.,
10 McDermott, F., and Spiro, B.: Controls on trace element (Sr-Mg) compositions of
11 carbonate cave waters: implications for speleothem climatic records, *Chem. Geol.*,
12 166, 255-269, 2000.

13 Faith, J. T.: Late Pleistocene and Holocene mammal extinctions on continental Africa,
14 *Earth-Sci. Rev.*, 128, 105-121, 2014.

15 Finné, M., Holmgren, K., Sundqvist, H. S., Weiberg, E., and Lindblom, M.: Climate
16 in the eastern Mediterranean, and adjacent regions, during the past 6000 years - A
17 review, *J. Archaeol. Sci.*, 38, 3153-3173, 2011.

18 Genty, D., Baker, A., Massault, M., Proctor, C., Gilmour, M., and Pons-Branchu, E.:
19 Dead carbon in stalagmites: Carbonate bedrock paleodissolution vs. ageing of soil
20 organic matter. Implications for ^{13}C variations in speleothems, *Geochim. Cosmochim.*
21 *Acta*, 65, 3443-3457, 2001a.

22 Genty, D., Baker, A., and Vokal, B.: Intra- and inter-annual growth rate of modern
23 stalagmites, *Chem. Geol.*, 176, 191-212, 2001b.

24 Genty, D., Labuhn, I., Hoffmann, G., Danis, P. A., Mestre, O., Bourges, F., Wainer, K.,

1 Massault, M., R égnier, E., Orengo, P., Falourd, S., and Minster, B.: Rainfall and cave
2 water isotopic relationships in two South-France sites, *Geochim. Cosmochim. Acta*,
3 131, 323-343, 2014.

4 Hendy, C. H.: The isotopic geochemistry of speleothems-I.The calculation of the
5 effects of different modes of formation on the isotopic composition of speleothems
6 and their applicability as palaeoclimatic indicators, *Geochim. Cosmochim. Acta*, 35,
7 801-824, 1971.

8 Hoerling, M. and Kumar, A.: The perfect ocean for drought, *Science*, 299, 691-694,
9 2003.

10 IAEA: Isotopic composition of precipitation in the Mediterranean Basin in relation to
11 air circulation patterns and climate: final report of a coordinated research project,
12 2000-2004. International Atomic Energy Agency, Vienna, Austria, 2005.

13 Jackson, M. G., Oskarsson, N., Tronnes, R. G., McManus, J. F., Oppo, D. W.,
14 Gronvold, K., Hart, S. R., and Sachs, J. P.: Holocene loess deposition in Iceland:
15 evidence for millennial-scale atmosphere-ocean coupling in the North Atlantic,
16 *Geology*, 33, 509-512, 2005.

17 Jaffey, A. H., Flynn, K. F., Glendenin, L. E., Bentley, W. C., and Essling, A. M.:
18 Precision measurement of half-lives and specific activities of ^{235}U and ^{238}U , *Phys. Rev.*
19 C, 4, 1889-1906, 1971.

20 Jalut, G., Esteban Amat, A., Bonnet, L., Gauquelin, T., and Fontugne, M.: Holocene
21 climatic changes in the Western Mediterranean, from south-east France to south-east
22 Spain, *Palaeogeogr. Palaeocl. Palaeoecol.*, 160, 255-290, 2000.

23 Johnson, K. R., Hu, C. Y., Belshaw, N. S., and Henderson, G. M.: Seasonal
24 trace-element and stable-isotope variations in a Chinese speleothem: The potential for
25 high-resolution paleomonsoon reconstruction, *Earth Planet. Sci. Lett.*, 244, 394-407,

1 2006.

2 Kaufman, A., Wasserburg, G. J., Porcelli, D., Bar-Matthews, M., Ayalon, A., and
3 Halicz, L.: U-Th isotope systematics from the Soreq cave, Israel and climatic
4 correlations, *Earth Planet. Sci. Lett.*, 156, 141-155, 1998.

5 Kherbouche, F., Hachi, S., Abdessadok, S., Sehil, N., Merzoug, S., Sari, L.,
6 Benchernine, R., Chelli, R., Fontugne, M., Barbaza, M., and Roubet, C.: Preliminary
7 results from excavations at Gueldaman Cave GLD1 (Akbou, Algeria), *Quat. Int.*, 320,
8 109-124, 2014.

9 Kröpelin, S., Verschuren, D., Lézine, A.-M., Eggermont, H., Cocquyt, C., Francus, P.,
10 Cazet, J.-P., Fagot, M., Rumes, B., Russell, J. M., Darius, F., Conley, D. J., Schuster,
11 M., Suchodoletz, H. v., and Engstrom, D. R.: Climate-Driven Ecosystem Succession
12 in the Sahara: The Past 6000 Years, *Science*, 320, 765-768, 2006.

13 Lachniet, M. S.: Climatic and environmental controls on speleothem oxygen-isotope
14 values, *Quat. Sci. Rev.*, 28, 412-432, 2009.

15 Magny, M., Combourieu-Nebout, N., Beaulieu, J. L. d., Bout-Roumazeilles, V.,
16 Colombaroli, D., Desprat, S., Francke, A., Joannin, S., Ortu, E., Peyron, O., Revel, M.,
17 Sadori, L., Siani, G., Sicre, M. A., Samartin, S., Simonneau, A., Tinner, W., Vanni ère,
18 Wagner, B., Zanchetta, G., Anselmetti, F., Brugiapaglia, E., Chapron, E., Debret,
19 M., Desmet, M., Didier, J., Essallami, L., Galop, D., Gilli, A., Haas, J. N., Kallel, N.,
20 Millet, L., Stock, A., Turon, J. L., and Wirth, S.: North-south palaeohydrological
21 contrasts in the central Mediterranean during the Holocene: tentative synthesis and
22 working hypotheses, *Clim. Past*, 9, 2043-2071, 2013.

23 Magny, M., Vanni ère, B., Calo, C., Millet, L., Leroux, A., Peyron, O., Zanchetta, G.,
24 La Mantia, T., and Tinner, W.: Holocene hydrological changes in south-western
25 Mediterranean as recorded by lake-level fluctuations at Lago Preola, a coastal lake in

1 southern Sicily, Italy, *Quat. Sci. Rev.*, 30, 2459-2475, 2011.

2 Martrat, B., Grimalt, J. O., Lopez-Martinez, C., Cacho, I., Sierro, F. J., Flores, J. A.,
3 Zahn, R., Canals, M., Curtis, J. H., and Hodell, D. A.: Abrupt temperature changes in
4 the Western Mediterranean over the past 250,000 years, *Science*, 306, 1762-1765,
5 2004.

6 Mayewski, P. A., Rohling, E. E., Stager, J. C., Karlén, W., Maasch, K. A., Meeker, L.
7 D., Meyerson, E. A., Gasse, F., Kreveld, S. V., Holmgren, K., Lee-Thorp, J., Rosqvist,
8 G., Rack, F., Staubwasser, M., Schneider, R. R., and Steig, E. J.: Holocene climate
9 variability, *Quat. Res.*, 62, 243- 255, 2004.

10 McDermott, F.: Palaeo-climate reconstruction from stable isotope variations in
11 speleothems: a review, *Quat. Sci. Rev.*, 23, 901-918, 2004.

12 McGee, D., deMenocal, P. B., Winckler, G., W. Stuut, J. B., and Bradtmiller, L. I.: The
13 magnitude, timing and abruptness of changes in North African dust deposition over
14 the last 20,000 yr, *Earth Planet. Sci. Lett.*, 371-372, 163-176, 2013.

15 Mickler, P. J., Banner, J. L., Stern, L., Asmeron, Y., Edwards, R. L., and Ito, E.: Stable
16 isotope variations in modern tropical speleothems: Evaluating equilibrium vs. kinetic
17 isotope effects, *Geochim. Cosmochim. Acta*, 68, 4381-4393, 2004.

18 Mickler, P. J., Stern, L. A., and Banner, J. L.: Large kinetic isotope effects in modern
19 speleothems, *Geol. Soc. Am. Bull.*, 118, 65-81, 2006.

20 Morrelon, M., zvalero-Garces, B., Vegas-Vilarrubia, T., Gonzalez-Samperiz, P.,
21 Romero, O., Delgado-Huertas, A., Mata, P., Moreno, A., Rico, M., and Corella, J. P.:
22 Lateglacial and Holocene paleohydrology in the western Mediterranean region: the
23 Lake Estanya record (NE Spain), *Quat. Sci. Rev.*, 28, 2582-2599, 2009.

24 Regattieri, E., Zanchetta, G., Drysdale, R. N., Isola, I., Hellstrom, J. C., and Dallai, L.:

1 Lateglacial to Holocene trace element record (Ba, Mg, Sr) from Carchia Cave (Apuan
2 Alps, central Italy): paleoenvironmental implications, *J. Quat. Sci.*, 29, 381-392,
3 2014.

4 Reimer, P. J., Bard, E., Bayliss, A., Beck, J. W., Blackwell, P. J., Bronk Ramsey, C.,
5 Buck, C. E., Cheng, H., Edwards, R. L., Friedrich, M., Grootes, P. M., Guilderson, T.
6 P., Haflidason, H., Hajdas, I., Hatté, C., Heaton, T. J., Hoffmann, D. L., Hogg, A. G.,
7 Hughen, K. A., Kaiser, K. F., Kromer, B., Manning, S. W., Niu, M., Reimer, R. W.,
8 Richards, D. A., Scott, E. M., Sounthor, J. R., Staff, R. A., Turney, C. S. M., and van
9 der Plicht, J.: IntCal13 and Marine13 radiocarbon age calibration curves 0-52,000
10 years cal BP, *Radiocarbon*, 55, 1869-1887, 2013.

11 Riehla, S., Pustovoytov, K. E., Weippert, H., Klett, S., and Hole, F.: Drought stress
12 variability in ancient Near Eastern agricultural systems evidenced by $\delta^{13}\text{C}$ in barley
13 grain, *PNAS*, 111, 12348-12353, 2014.

14 Roberts, N., Brayshaw, D., Kuzucuoglu, C., Perez, R., and Sadori, L.: The
15 mid-Holocene climatic transition in the Mediterranean: Causes and consequences,
16 *The Holocene*, 21, 3-13, 2011.

17 Roland, T. P.: Was there a '4.2 kyr event' in Great Britain and Ireland? Evidence from
18 the peatland record, PhD, University of Exeter, Exeter, UK, 2012.

19 Sadori, L. and Giardini, M.: Charcoal analysis, a method to study vegetation and
20 climate of the Holocene: The case of Lago di Pergusa (Sicily, Italy). *Geobios*, 40,
21 173-180, 2007.

22 Sadori, L., Jahns, S., and Peyron, O.: Mid-Holocene vegetation history of the central
23 Mediterranean, *The Holocene*, 21, 117-129, 2011.

24 Sadori, L. and Narcisi, B.: The postglacial record of environmental history from Lago
25 di Pergusa, Sicily, *The Holocene*, 11, 655-672, 2001.

1 Scholz, D. and Hoffmann, D. L.: StalAge - An algorithm designed for construction of
2 speleothem age models, *Quat. Geochronol.*, 6, 369-382, 2011.

3 Seager, R., Ting, M., Held, I., Kushnir, Y., Lu, J., Vecchi, G., Huang, H. P., Harnik, N.,
4 Leetmaa, A., Lau, N. C., Li, C., Velez, J., and Naik, N.: Model projections of an
5 imminent transition to a more arid climate in southwestern North America, *Science*,
6 316, 1181-1184, 2007.

7 Staubwasser, M., Sirocko, F., Grootes, P., and Segl, M.: Climate change at the 4.2 ka
8 BP termination of the Indus valley civilization and Holocene south Asian monsoon
9 variability, *Geophys. Res. Lett.*, 30, 1-4, 2003.

10 Staubwasser, M. and Weiss, H.: Holocene climate and cultural evolution in late
11 prehistoric–early historic West Asia, *Quat. Res.*, 66, 372-378, 2006.

12 Stoll, H. M., Moreno, A., Mendez-Vicente, A., Gonzalez-Lemos, S., Jimenez-Sanchez,
13 M., Dominguez-Guesta, M. J., Edwards, R. L., Cheng, H., and Wang, X.:
14 Paleoclimate and growth rates of speleothems in the northwestern Iberian peninsula
15 over the last two glacial cycles, *Quat. Res.*, 80, 284-290, 2013.

16 Tindall, J. C. and Valdes, P. J.: Modeling the 8.2 ka event using a coupled
17 atmosphere-ocean GCM, *Global Planet. Change*, 79, 312-321, 2011.

18 Touchan, R., Anchukaitis, K. J., Meko, D. M., Attalah, S., Baisan, C., and Aloui, A.:
19 Long term context for recent drought in northwestern Africa, *Geophys. Res. Lett.*, 35,
20 10.1029/2008GL034264, 2008.

21 Touchan, R., Anchukaitis, K. J., Meko, D. M., Sabir, M., Attalah, S., and Aloui, A.:
22 Spatiotemporal drought variability in northwestern Africa over the last nine centuries,
23 *Clim. Dyn.*, 37, 237-252, 2011.

24 Vaks, A., Woodhead, J., Bar-Matthews, M., Ayalon, A., Cliff, R. A., Zilberman, T.,

1 Matthews, A., and Frumkin, A.: Pliocene–Pleistocene climate of the northern margin
2 of Saharan–Arabian Desert recorded in speleothems from the Negev Desert, Israel,
3 *Earth Planet. Sci. Lett.*, 368, 88-100, 2013.

4 Wanner, H., Beer, J., Büikofer, J., Crowley, T. J., Cubasch, U., Flückiger, J., Goosse,
5 H., Grosjean, M., Joos, F., Kaplan, J. O., Küttel, M., Müller, S. A., Prentice, C. I.,
6 Solomina, O., Stocker, T. F., Tarasov, P., Wagner, M., and Widmann, M.: Mid- to Late
7 Holocene climate change: an overview, *Quat. Sci. Rev.*, 27, 1791-1828, 2008.

8 Weiss, H. and Bradley, R. S.: What Drives Societal Collapse?, *Science*, 291, 609-610,
9 2000.

10 Weiss, H., Courty, M.-A., Wetterstrom, W., Guichard, F., L.Senior, Meadow, R., and
11 A.Curnow: The genesis and collapse of third millennium North Mesopotamian
12 civilization, *Science*, 261, 995-1004, 1993.

13 Wiener, M. H.: The interaction of climate change and agency in the collapse of
14 civilizations ca. 2300-2000 BC, *Radiocarbon*, 56, 10.2458/azu_rc.2456.18325, 2014.

15 Zanchetta, G., Bar-Matthews, M., Drysdale, R. N., Lionello, P., Ayalon, A., Hellstrom,
16 J. C., Isola, I., and Regattieri, E.: Coeval dry events in the central and eastern
17 Mediterranean basin at 5.2 and 5.6 ka recorded in Corchia (Italy) and Soreq caves
18 (Israel) speleothems, *Global Planet. Change*, 122, 130-139, 2014.

19 Zanchetta, G., Drysdale, R. N., Hellstrom, J. C., Fallick, A. E., Isola, I., Gagan, M. K.,
20 and Paresch, M. T.: Enhanced rainfall in the Western Mediterranean during deposition
21 of sapropel S1: stalagmite evidence from Corchia cave (Central Italy), *Quat. Sci. Rev.*,
22 26, 279-286, 2007.

23 Zanchetta, G., Giraudi, C., Sulpizio, R., Magny, M., Drysdale, R. N., and Sadori, L.:
24 Constraining the onset of the Holocene "Neoglacial" over the central Italy using
25 tephra layers, *Quat. Res.*, 78, 236-247, 2012a.

1 Zanchetta, G., van Welden, A., Baneschi, I., Drysdale, R. N., Sadori, L., Roberts, N.,
2 Giardini, M., Beck, C., and Pascucci, V.: Multiproxy record for the last 4500 years
3 from Lake Shkodra (Albania/Montenegro), *J. Quat. Sci.*, 27, 780-789, 2012b.

4

5

1 Table 1. U/Th dates from MC-ICP-MS analyses of stalagmites GLD1-stm2 and GLD1-stm4 from the Gueldaman GLD1 Cave. Analytical errors
 2 are 2σ of the mean. U decay constants: $\lambda_{238} = 1.55125 \times 10^{-10}$ (Jaffey et al., 1971) and $\lambda_{234} = 2.82206 \times 10^{-6}$ (Cheng et al., 2013). Th decay constant:
 3 $\lambda_{230} = 9.1705 \times 10^{-6}$ (Cheng et al., 2013). * $\delta^{234}\text{U} = ([^{234}\text{U}/^{238}\text{U}]_{\text{activity}} - 1) \times 1000$. ** $\delta^{234}\text{U}_{\text{initial}}$ was calculated based on ^{230}Th age (T), i.e., $\delta^{234}\text{U}_{\text{initial}} = \delta^{234}\text{U}_{\text{measured}} \times e^{\lambda^{234}\text{U} \times T}$. Corrected ^{230}Th ages assume the initial $^{230}\text{Th}/^{232}\text{Th}$ atomic ratio of $4.4 \pm 2.2 \times 10^{-6}$. Those are the values for a
 4 material at secular equilibrium, with the bulk earth $^{232}\text{Th}/^{238}\text{U}$ value of 3.8. The errors are arbitrarily assumed to be 50%. ***BP stands for
 5 “Before Present” where the “Present” is defined as the year 2000 AD.
 6

Sample	^{238}U	^{232}Th	$^{230}\text{Th} / ^{232}\text{Th}$	$d^{234}\text{U}^*$	$^{230}\text{Th} / ^{238}\text{U}$	^{230}Th Age	^{230}Th Age	$d^{234}\text{U}_{\text{Initial}}^{**}$	^{230}Th Age	Laboratory
Number	(ppb)	(ppt)	(atomic)	(measured)	(activity)	(uncorrected)	(corrected)	(corrected)	(corrected)	
$\times 10^{-6}$										
GLD1-stm2-7	169	± 0.1	396	± 0	136	± 1	863	± 2.3	0.105	± 0.001
GLD1-stm2-36	154	± 0.2	1922	± 39	137	± 3	910	± 2.2	0.103	± 0.000
GLD1-stm2-98	150	± 0.2	69	± 2	3077	± 73	776	± 2.4	0.086	± 0.000
GLD1-stm2-180	152	± 0.2	161	± 3	1157	± 25	644	± 2.0	0.074	± 0.000
GLD1-stm2-192	162	± 0.1	182	± 4	1158	± 24	807	± 1.7	0.079	± 0.000
GLD1-stm2-213	175	± 0.2	547	± 11	390	± 8	697	± 2.0	0.074	± 0.000
							4841	± 33	4788	± 50
									707	± 2.1
										4775 ± 50
										UM

GLD1-stm2-286	169	± 0.2	207	± 4	980	± 21	756	± 1.8	0.073	± 0.000	4601	± 25	4581	± 28	765	± 1.9	4568	± 28	UM
GLD1-stm2-320	195	± 0.3	384	± 8	575	± 12	759	± 2.2	0.069	± 0.000	4321	± 26	4288	± 34	769	± 2.2	4276	± 34	Xi'an U
GLD1-stm2-340	194	± 0.3	354	± 7	612	± 13	800	± 2.9	0.068	± 0.000	4172	± 20	4142	± 29	809	± 2.9	4129	± 29	UM
GLD1-stm4-10	105	± 0.1	283	± 6	415	± 11	322	± 1.5	0.068	± 0.001	5734	± 90	5675	± 99	327	± 1.6	5662	± 99	UM
GLD1-stm4-24	126	± 0.1	983	± 20	135	± 3	347	± 1.9	0.064	± 0.001	5311	± 49	5143	± 128	352	± 1.9	5131	± 128	Xi'an U
GLD1-stm4-30	106	± 0.1	1362	± 27	80	± 2	298	± 1.9	0.062	± 0.001	5321	± 57	5035	± 210	302	± 1.9	5023	± 210	Xi'an U
GLD1-stm4-47	96	± 0.1	1104	± 22	88	± 2	290	± 1.9	0.062	± 0.001	5341	± 63	5082	± 194	294	± 1.9	5070	± 194	Xi'an U
GLD1-stm4-70	224	± 0.4	749	± 15	254	± 5	334	± 2.5	0.051	± 0.000	4282	± 27	4210	± 58	338	± 2.6	4197	± 58	UM
GLD1-stm4-113	155	± 0.2	130	± 3	910	± 20	363	± 2.1	0.046	± 0.000	3761	± 29	3743	± 32	367	± 2.1	3730	± 32	UM
GLD1-stm4-152	180	± 0.3	582	± 12	226	± 5	373	± 2.0	0.045	± 0.000	3590	± 25	3521	± 54	376	± 2.0	3508	± 54	UM
GLD1-stm4-195	175	± 0.1	929	± 19	131	± 4	369	± 1.7	0.042	± 0.001	3403	± 74	3290	± 108	372	± 1.8	3277	± 108	UM

1 Table 2. Radiocarbon dates from AMS analyses of charcoals from excavation sector S2
 2 inside the Gueldaman GLD1 Cave. * Kherbouche et al. (2014). Ages are reported in
 3 years before 2000 AD.

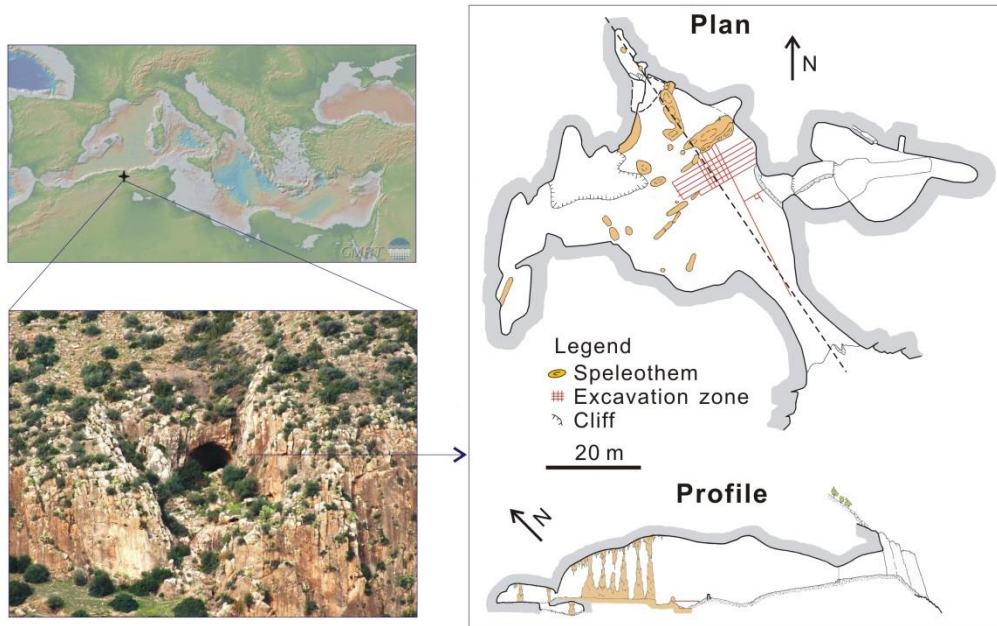
Depth Z (cm)	Square	Lab No. (SacA#)	Material	14C Age ($\pm 2\sigma$; yr)	Median Age (yr)	Cal. Interval (2σ ; yr)	Note
60	M48	39408	Charcoal	1600 \pm 30	1482	1385 - 1604	This study
65	N48	29731	Charcoal	1610 \pm 25	1484	1415 - 1547	*
84	N48	39410	Charcoal	4020 \pm 30	4495	4411 - 4785	This study
86	N48	39411	Charcoal	3975 \pm 30	4416	4290 - 4569	This study
91	M48	39409	Charcoal	3945 \pm 30	4403	4244 - 4522	This study
108	N47	36982	Charcoal	4355 \pm 30	4918	4851 - 5032	This study
124	L48	23883	Charcoal	5250 \pm 35	6003	5924 - 6178	*
132	L48	23884	Charcoal	4260 \pm 30	6025	5933 - 6178	*
147	M47	36981	Charcoal	6120 \pm 35	7002	6907 - 7157	This study

4

1 Table 3. Summary of the features of climate and human activity in different climate
 2 periods and occupation phases.

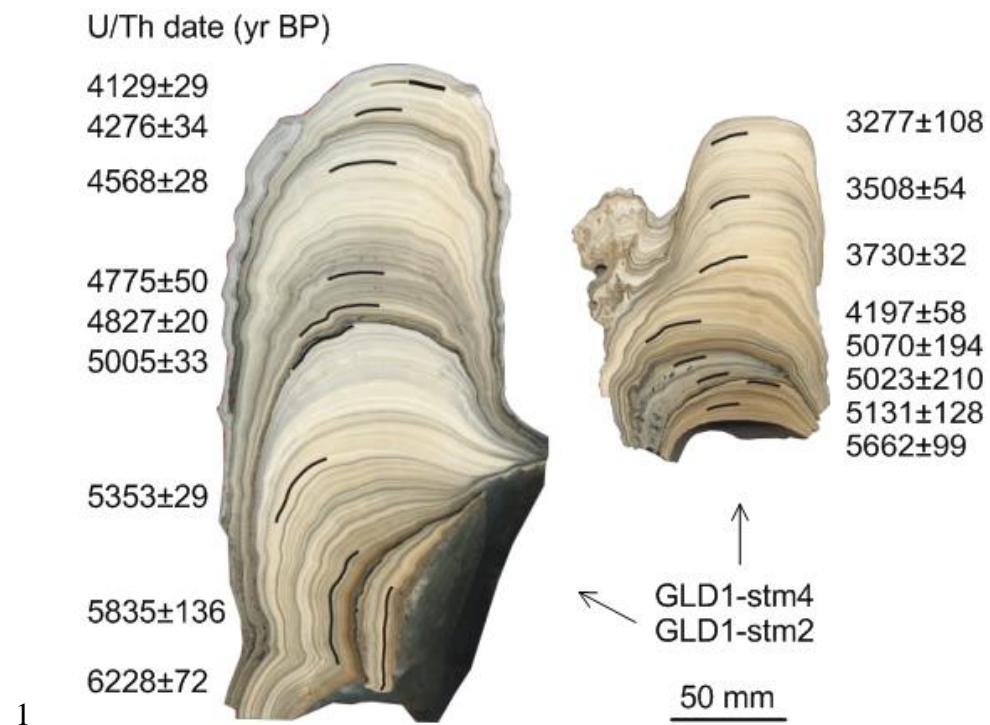
Climate period	Age (yr)	^{230}Th	Climate condition	Occupation phase	Age (cal yr)	^{14}C	Human activity
/	/	/		0	~7002-6003		Permanent and intensive occupation
1	~6200-5100	Wet & oscillatory		1	~6003-4918		Permanent but less intensive occupation
2	~5100-4400	dramatic shift in the 2 last ~200 years			~4918-4403		Permanent and most intensive occupation
3	~4400-3800	Extremely dry		3	~4403-1484		Abandonment of the cave/occasional visit
4	~3800-3200	Relatively wetter		4	~1484-		Re-occupation of the cave

3

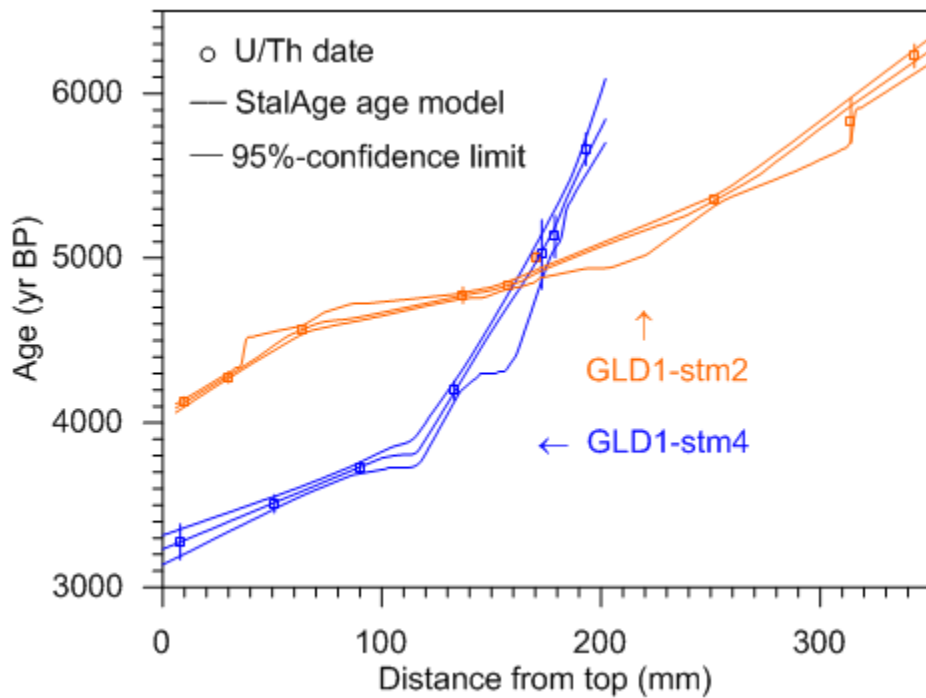


1

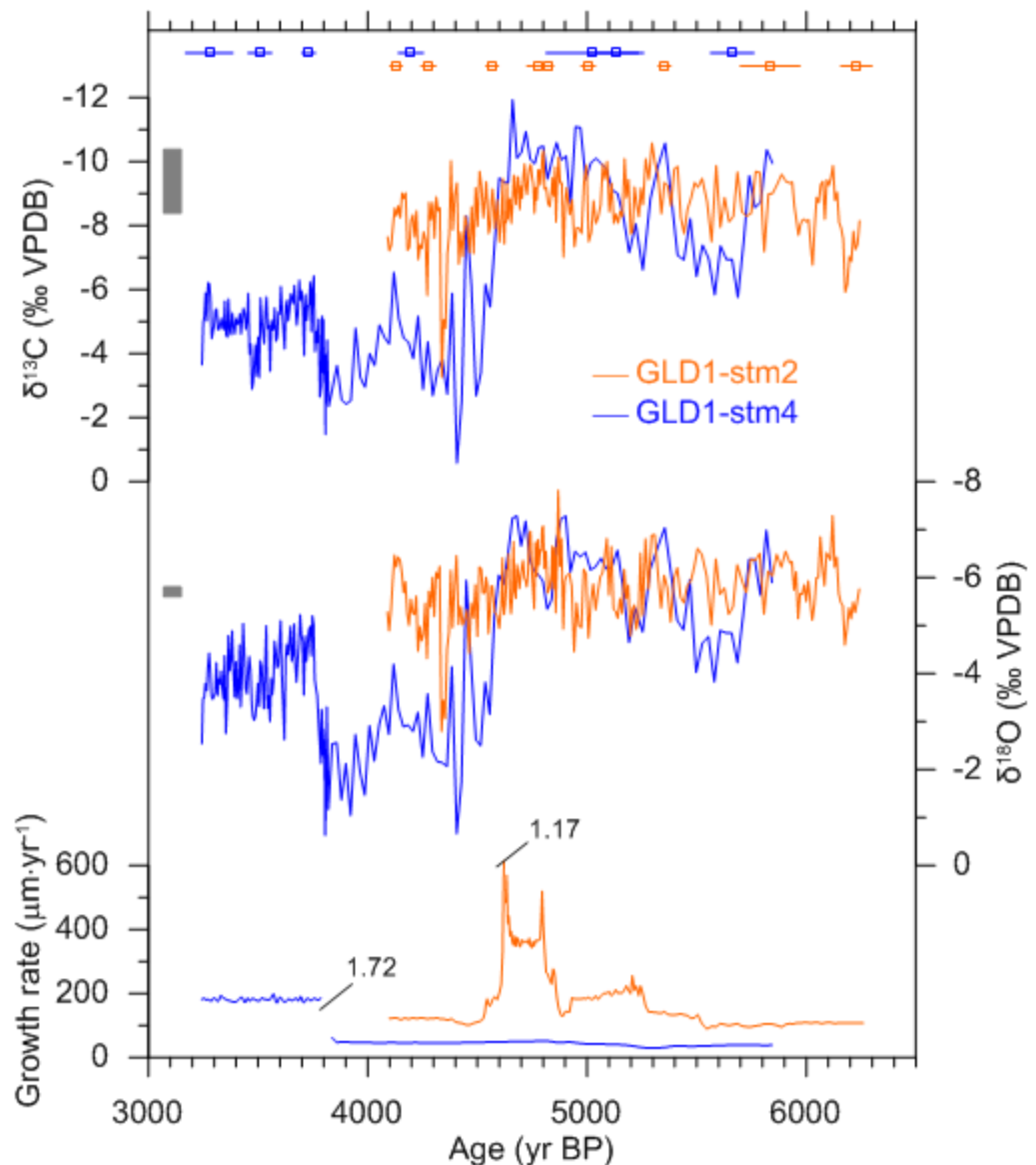
2 Figure 1. The Gueldaman GLD1 Cave ($36^{\circ}26'N$, $4^{\circ}34'E$, 507 m asl). The top left
 3 shows the location of the Gueldaman GLD1 Cave, in the N-Algeria of
 4 W-Mediterranean basin; the low left shows a photo of cave entrance and local
 5 vegetation cover; the right panel shows maps of inner cave where stalagmites and
 6 archaeological deposits are collected.



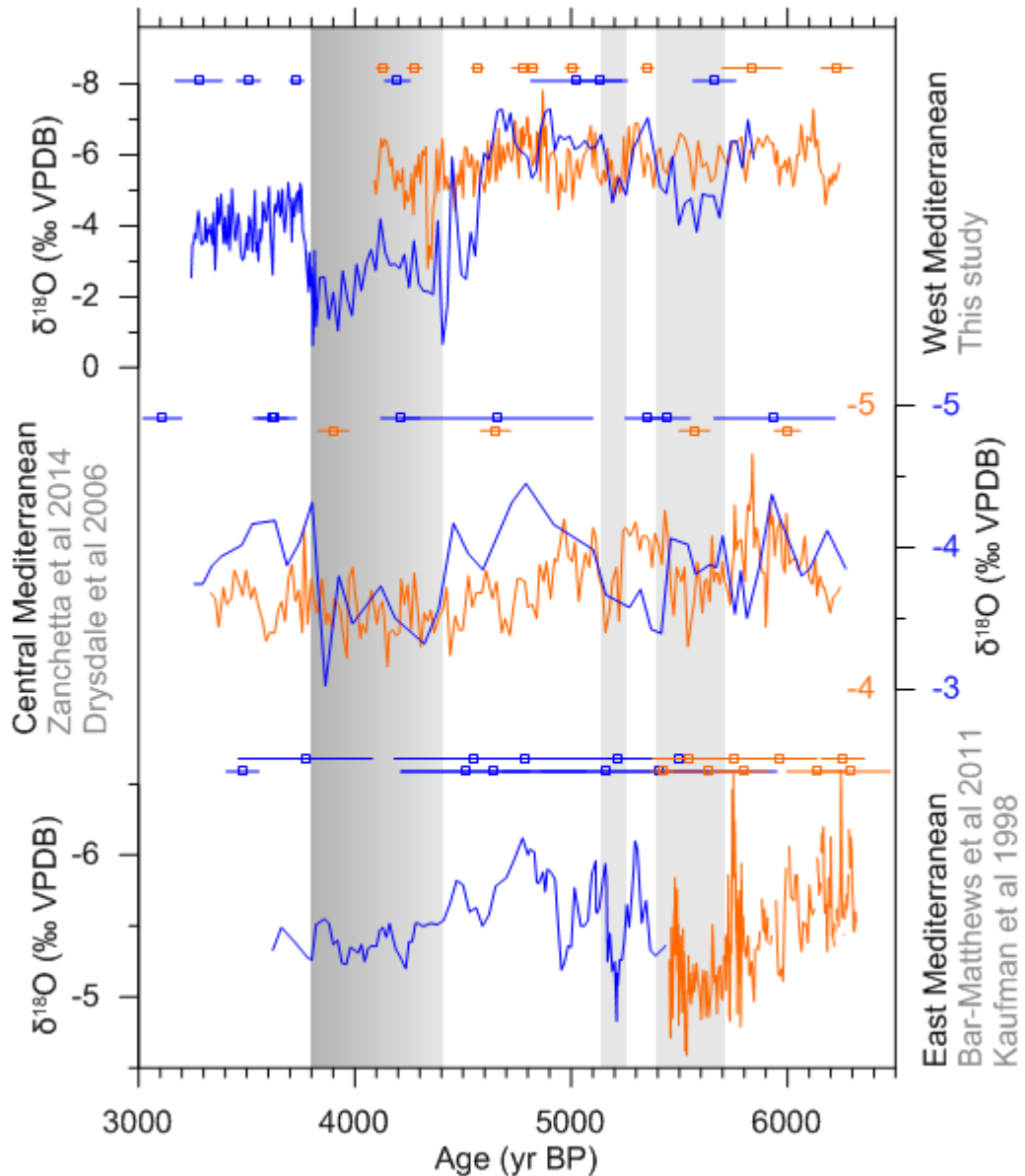
2 Figure 2. U/Th dating of stalagmites GLD1-stm2 and GLD1-stm4 from the Gueldaman
3 GLD1 Cave. U/Th dates and 2 σ errors are shown next to sampling positions.



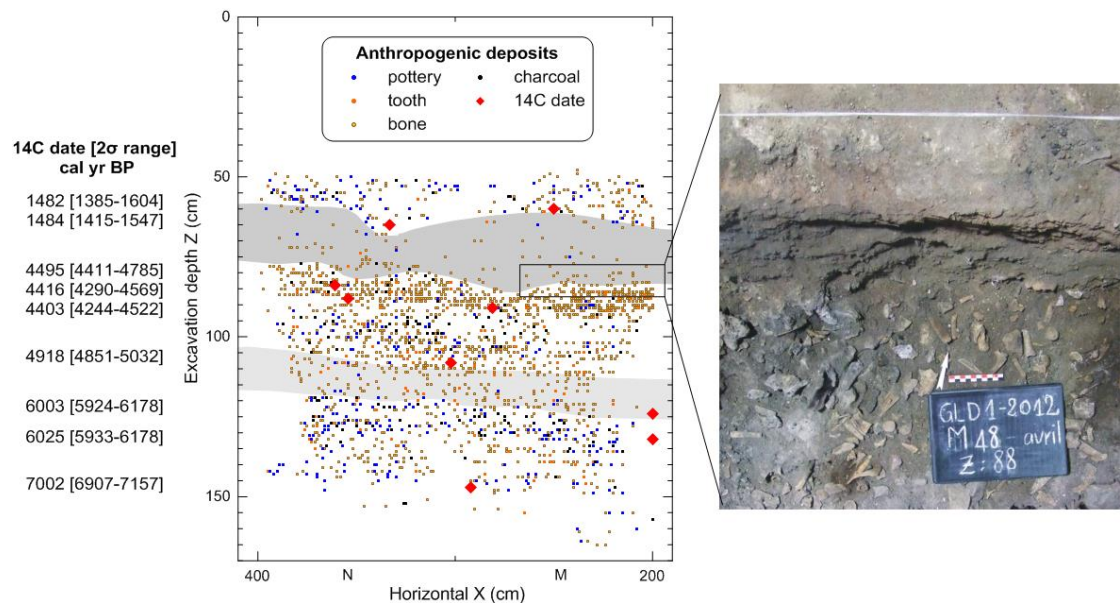
1
 2 Figure 3. Age models of stalagmites GLD1-stm2 and GLD1-stm4 from the Gueldaman
 3 GLD1 Cave. The age models were calculated using the StalAge program (Scholz and
 4 Hoffmann, 2011). Note that the U/Th date of sample GLD1-stm4-47 was detected as a
 5 major outlier and not used in the final age model of stalagmite GLD1-stm4. The 2σ
 6 analytical uncertainty of each U/Th date (dot) is represented by the error bars,
 7 whereas the 95% uncertainty assessed from the model simulation is represented by
 8 thin curves.



1 Figure 4. The $\delta^{18}\text{O}$, $\delta^{13}\text{C}$ and growth rate of stalagmites GLD1-stm2 and GLD1-stm4
 2 from the Gueldaman GLD1 Cave. U/Th dates with 2σ errors are presented at the top.
 3 The isotopic ranges of modern calcites are also shown on the left (rectangles). Growth
 4 rates are calculated from the StalAge age model. Note that the extraordinarily high
 5 growth at ca. 4600 yr BP in stalagmite GLD1-stm2 and ca. 3800 yr BP in stalagmite
 6 GLD1-stm4 are likely attributed to artificial simulations by the StalAge program and
 7 thus are not fully discussed in terms of climate in the text.

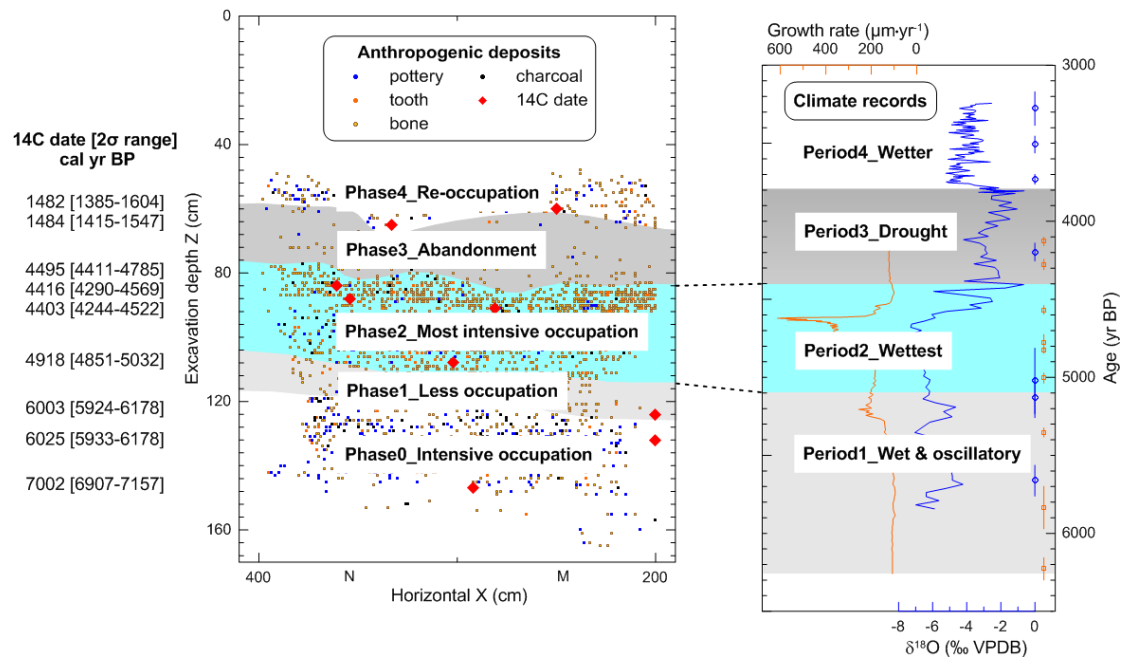


1
 2 Figure 5. Comparison of high-resolution Mid-Holocene stalagmite $\delta^{18}\text{O}$ records across
 3 the Mediterranean basin. From the top to bottom are stalagmite records from the
 4 Gueldaman GLD1 Cave in N-Algeria of W-Mediterranean basin (this study), the
 5 Corchia Cave (Zanchetta et al., 2014) and the Renella Cave (Drysdale et al., 2006) in
 6 Central Italy of Central Mediterranean basin, and the Soreq Cave (Bar-Matthews and
 7 Ayalon, 2011; Kaufman et al., 1998) in Israel of E-Mediterranean basin. Different
 8 stalagmites from each area are represented in distinct colors. U/Th dates with 2σ
 9 errors are shown at the top of each curve. Ages are reported in years before 2000 AD.



1

2 Figure 6. Radiocarbon dating of anthropogenic deposits layers in excavation sector S2
 3 inside the Gueldaman GLD1 Cave. From the left to right are ^{14}C dates of charcoal
 4 samples, anthropogenic deposit distribution, and a photo at depth across $\sim 75\text{-}88$ cm
 5 showing a transition of layer from rich to rare anthropogenic deposits. The gray
 6 colour highlights two phases with diminished anthropogenic remains (especially
 7 pottery and charcoal) at ca. 4403-1484 cal yr BP (depths of $\sim 75\text{-}60$ cm) and ca.
 8 6003-4918 cal yr BP (depths of $\sim 120\text{-}105$ cm).



1

2 Figure 7. Comparison between evidence of ancient human occupation and of past
3 climate change from the Gueldaman GLD1 Cave. The definition of occupation phases
4 0-4 and climate periods 1-4 are referred to the text.